Biochemical and Biophysical Research Communications 433 (2013) 573–578

Contents lists available at SciVerse ScienceDirect

Biochemical and Biophysical Research Communications

journal homepage: www.elsevier.com/locate/ybbrc

# Antiproliferative effects of phenylaminonaphthoquinones are increased by ascorbate and associated with the appearance of a senescent phenotype in human bladder cancer cells

K.B. Felipe [a], J. Benites [b], C. Glorieux [c], B. Sid [c], M. Valenzuela [c], M.R. Kviecinski [a], R.C. Pedrosa [a], J.A. Valderrama [d], Ph. Levêque [e], B. Gallez [e], J. Verrax [c], P. Buc Calderon [b,c,*]

[a] Laboratorio de Bioquímica Experimental, Departamento de Bioquímica, Universidade Federal de Santa Catarina, Florianópolis, Brasil
[b] Facultad de Ciencias de la Salud, Universidad Arturo Prat, Avenida Arturo Prat 2120, Casilla 121, Iquique, Chile
[c] Université Catholique de Louvain, Louvain Drug Research Institute, Toxicology and Cancer Biology Research Group (GTOX), Brussels, Belgium
[d] Departamento Química Orgánica, Pontificia Universidad Católica de Chile, Vicuña Mackenna 4860, Casilla 306, Santiago, Chile
[e] Université Catholique de Louvain, Louvain Drug Research Institute, Biomedical Magnetic Resonance Research Group (REMA), Brussels, Belgium

ARTICLE INFO

*Article history:*
Received 8 March 2013
Available online 22 March 2013

*Keywords:*
Ascorbate
Cell proliferation
Naphthoquinones
Senescence
T24 bladder cancer cells

ABSTRACT

Quinone-containing molecules have been developed against cancer mainly for their redox cycling ability leading to reactive oxygen species (ROS) formation. We have previously shown that donor-acceptor phenylaminonaphthoquinones are biologically active against a panel of cancer cells. In this report, we explored the mechanisms involved in cancer cell growth inhibition caused by two phenylaminonaphthoquinones, namely **Q7** and **Q9**, with or without ascorbate (ASC). The results show that **Q7** and **Q9** are both redox cyclers able to form ROS, which strongly inhibit the proliferation of T24 cells. **Q9** was a better redox cycler than **Q7** because of marked stabilization of the semiquinone radical species arising from its reduction by ascorbate. Indeed, ASC dramatically enhances the inhibitory effect of **Q9** on cell proliferation. **Q9** plus ASC impairs the cell cycle, causing a decrease in the number of cells in the G2/M phase without involving other cell cycle regulating key proteins. Moreover, **Q9** plus ASC influences the MAPK signaling pathways, provoking the appearance of a senescent cancer cell phenotype and ultimately leading to necrotic-like cell death. Because cellular senescence limits the replicative capacity of cells, our results suggest that induction of senescence may be exploited as a basis for new approaches to cancer therapy.


## 1. Introduction

Cancer is a major health problem affecting humans. Nearly 15 million new cases are diagnosed globally every year [1], but the use of conventional cancer chemotherapy is limited because of its toxic side effects [2].

As part of our ongoing studies concerning the preparation of potential biologically active compounds [3–5], we were interested in the synthesis of diversely substituted donor–acceptor phenylaminonaphthoquinones. Briefly, using an MTT-based screening assay, we have shown that these compounds are biologically active against a panel of cancer cells. Among this series, two quinones (namely **Q7** and **Q9**) markedly impaired the cellular ability to reduce MTT in three different cancer cell lines, while having a low cytotoxicity on healthy fibroblasts [4]. Previous data also have shown that the association of ascorbate (ASC) with some quinone-containing compounds potentiates their antitumor activity [3,6,7].

Because ascorbate enhances the redox cycling of menadione (a 1,4-naphthoquinone) leading to activation of the p38 MAPK pathway in breast MCF-7 cancer cells [8], we hypothesized about a potential involvement of this pathway in the mechanisms by which phenylaminonaphthoquinones cause cell growth arrest. On the other hand, the enzymatic cascades of ERK1/2 and p38 MAPK have been reported to be involved in premature senescence [9,10]. Cellular senescence is a growth-arrest program that limits the lifespan of mammalian cells and prevents unlimited cell proliferation [11]. Interestingly, when apoptosis fails to induce cancer cell death, the induction of cellular senescence is attractive because of its relationship with tumor suppression.

The aim of this paper was, therefore, to explore the effects of phenylaminonaphthoquinones, alone or associated with ascorbate (ASC), on cancer cell growth and cellular senescence. We describe the antiproliferative effects and the senescent phenotype induced by the selected quinones, namely **Q7** [2-(4-hydroxyanilino)-1,4-

* Corresponding author at: Université Catholique de Louvain, Louvain Drug Research Institute, Toxicology and Cancer Biology Research Group (GTOX), Brussels, Belgium. Fax: +32 2 7647359.
*E-mail address:* pedro.buccalderon@uclouvain.be (P. Buc Calderon).

0006-291X/$ - see front matter © 2013 Elsevier Inc. All rights reserved.
http://dx.doi.org/10.1016/j.bbrc.2013.03.028

naphthoquinone] and **Q9** [2-(4-methoxyanilino)-1,4-naphthoquinone], in T24 bladder carcinoma cells. We also report their effects on MAPK signaling pathways and on cancer cell survival.

## 2. Material and methods

### 2.1. Chemicals and antibodies

Quinones **Q7** [2-(4-hydroxyanilino)-1,4-naphthoquinone] and **Q9** [2-(4-methoxyanilino)-1,4-naphthoquinone] were synthesized by amination of 1,4-naphthoquinone with the respective arylamines, under aerobic conditions, using $CeCl_3 \cdot 7H_2O$ as the Lewis acid catalyst as previously described [4]. Dulbecco's modified Eagle medium (DMEM), fetal bovine serum (FBS) and antibiotics were purchased from Gibco (USA). Sodium ascorbate, bovine serum albumin (BSA), nocodazole and the protease inhibitor cocktail were purchased from Sigma–Aldrich (USA). MAPK inhibitors PD98054, SB202190, and SP600125 were from Calbiochem (Millipore). The 7-amino-4-trifluoromethylcoumarin conjugated (Ac-DEVD-AFC) was from Enzo Life Sciences (USA). The phosphatase inhibitor cocktail was from Calbiochem (Merck Biosciences). JNK, p38 and ERK1/2 antibodies were purchased from Cell Signaling Technology (USA). Survivin, p53, p27, p21 and rabbit polyclonal antibody against poly (ADP-ribose) polymerase (PARP) were from Santa Cruz Biotechnology, Inc. (USA). Secondary antibodies were from Dako (Denmark) and Chemicon (Millipore, USA). All other chemicals were made from ACS grade reagents.

### 2.2. Cell culture

The human bladder carcinoma T24 cells were a gift from Dr. F. Brasseur (Ludwig Institute for Cancer Research-Brussels). They were cultured as previously described [6].

### 2.3. Cell viability

Cytotoxicity was measured using MTT [12] and trypan blue [13] assays. For the MTT assay, $10^4$ cells/well were plated onto 96-well plates and, after confluence, cells were treated for 24 h with the respective treatments. Cells were then washed twice with PBS and incubated for 2 h with MTT (0.5 mg/mL). Formazan crystals were solubilized by adding DMSO (100 μL/well) and the colored solutions were read at 550 nm. To verify the involvement of MAPK in the cytotoxicity, cells were pretreated for 2 h with the following MAPK inhibitors: (a) PD98054 (10 μM), (b) SB202190 (10 μM), (c) SP600125 (20 μM).

The Trypan blue assay was performed after a 24 h-exposure of T24 cells to quinones (10 μM), alone or with ASC (1 mM). After staining, cells were counted by a TC10 automated cell counter (Bio-Rad, USA), and the percentage cell viability was determined.

### 2.4. Cell cycle analysis

Cells were plated into 6-well plates ($50–100 \times 10^3$) and synchronized with nocodazole (30 ng/ml) for 14 h. Cells were treated for up to 72 h with the respective treatments. Cells were then washed and the cell pellet was resuspended in ice-cold 80% ethanol and kept at −20 °C overnight. Finally, cells were washed again with PBS and incubated for 20 min in a saponin-based permeabilization solution (BSA 1%, ribonuclease A 0.2 mg/ml and propidium iodide 50 μg/ml). Flow cytometry was performed using an LSRFortessa (BD Biosciences) FACS data were analyzed using the FlowJo software (Treestar).

### 2.5. Immunoblotting assays

After treatments, cells were washed with PBS and lysed in RIPA buffer (50 mM Tris–Cl pH 7.4, 150 mM NaCl, 1% NP40, 0.25% Na-deoxycholate and 1 mM phenylmethylsulfonyl fluoride) supplemented with 1% protease inhibitor and 3% phosphatase inhibitor cocktails. After denaturation in Laemmli buffer (60 mM Tris–Cl pH 6.8, 2% SDS, 10% glycerol, 5% β-mercaptoethanol, 0.01% bromophenol blue), equal amounts of protein (30 μg) were subjected to SDS–PAGE electrophoresis followed by electroblot to nitrocellulose membranes. After blocking and washing, the membranes were incubated overnight with the primary antibodies, washed again and further incubated with the secondary antibodies. Immunodetection was performed using the enhanced chemiluminescence (ECL) detection kit (Amersham, UK) for HRP-coupled secondary antibodies. β-Actin served as a loading control.

### 2.6. Caspase-3 activity

After treatments, cells were washed twice with PBS, lysed, centrifuged, and the supernatants were incubated with the fluorogenic caspase-3 substrate, Ac-DEVD-AFC. Fluorochrome release after peptide cleavage was determined kinetically at room temperature using a Victor X2 spectrophotometer at $\lambda = 380$ nm for excitation and $\lambda = 505$ nm for emission (Perkin Elmer, Waltham, USA). Results are expressed as Units/mg protein, as originally described by Nicholson et al. [14]. Sanguinarine (5 μM), a flavonoid known to induce apoptosis [15], was used as a positive control.

### 2.7. Colony formation assay

The potential to induce clonogenic death was evaluated according to Franken et al. [16]. Cells (500/well) were treated for 24 h with the respective treatments. They were then washed twice with warm PBS and fresh medium was added. After 10–12 days, cells were stained with crystal violet and colonies with more than 50 cells were counted.

### 2.8. Electron paramagnetic resonance (EPR)

Phenylaminonaphthoquinones and ASC were solubilized at 10–100 μM and 1 mM, respectively. EPR spectra were obtained at X-band (9.785 GHz) on a Bruker EMX spectrometer equipped with a variable temperature controller, BVT-3000, using 5 mW microwave power, a modulation frequency of 100 kHz and a modulation amplitude of 0.63 G. The recording of EPR spectra was started 1 min after inserting a sample into the cavity. The scan time was 20.9 s. All spectra were collected at 37 °C as previously reported [7].

### 2.9. Senescence assays

Cells were exposed for 24 h to **Q7** (10 μM) or **Q9** (4 μM), alone or with 1 mM ASC. Induction of senescence was assessed by measuring SA-β-galactosidase (β-Gal) activity using the senescence cells histochemical staining kit from Sigma–Aldrich (USA) and according to the procedures described by the manufacturer. Cell staining and morphology were assessed by microscopy. Images were captured by the Motics Image Plus 2.0 software (Ted Pella Inc., Redding, USA). We used an arbitrary quantitative analysis to record the number of β-Gal positive stained cells in each experimental condition. Briefly, β-Gal positive cells were counted by analyzing approximately 30 cells for each magnified field (X) and 10 fields were taken into account. Data were recorded as percentage of senescent cells.

The role of MAPK in cell senescence was evaluated using the MAPK inhibitors previously reported for the cytotoxicity assays (point 2.3).

### 2.10. Data analysis

The *in vitro* assays were performed in triplicate and repeated three times independently. Data were recorded as means ± standard deviation or percentages. Data were analyzed by the ANOVA test followed by the Bonferroni test. Comparisons were assessed using GraphPad Prism software (San Diego, USA). Values of $p < 0.05$ were considered to be statistically significant.

## 3. Results

### 3.1. Ascorbate-driven Q7/Q9-redox cycling inhibits cell growth and induces necrotic-like cell death in T24 cells

T24 cells treated for 24 h with **Q7** or **Q9** loss their ability to reduce MTT and ASC enhanced this quinone cytotoxicity (Fig. 1a). In the case of **Q9** + ASC, the decreased ability to reduce MTT may be associated with a cytolytic effect, as shown by the almost 40% cell death shown using the Trypan blue exclusion test (Fig. 1b). The cell death is likely to have been necrosis, because we were unable to detect any caspase activation in cells incubated with quinones alone or with ASC either by immunoblotting to detect the cleavage of the PARP protein, a well-known substrate of caspase-3 (Fig. 1c), or using a fluorochrome substrate (DEVDase activity) indicating peptide cleavage (Supplementary Table 1S). In contrast, sanguinarine provoked the cleavage of both the DEVD peptide and the PARP protein.

A potentiating effect of ASC was also observed on cell proliferation, as measured by a clonogenic assay (Fig. 2a and b). The antiproliferative effect of **Q9** (1 μM) was stronger than that of **Q7** (2.5 μM), regardless of the absence or presence of ASC. Indeed, **Q9** + ASC inhibited cell growth by 85% compared to **Q7** + ASC, which inhibited cell growth by only 35%. ASC thus enhances quinone redox cycling, likely as a result of its reducing power. To confirm this effect, we analyzed the formation of ascorbyl radical using EPR spectroscopy (Fig. 2c). According to the previous hypothesis and in agreement with the above results, the association of **Q9** + ASC showed an EPR signal corresponding to ascorbyl radical with a stronger intensity than that produced by **Q7** + ASC. Indeed, compared to the signal detected in the presence of ASC alone, **Q9** + ASC increased the signal by 4.5-fold whereas **Q7** + ASC increased it only 3.5-fold.

### 3.2. Quinones plus ASC affect the distribution of cells across the cell cycle without changes in the amount of key proteins regulating the cell cycle at different check points

Because of the remarkable inhibitory effect of phenylaminonaphthoquinones plus ASC on cancer cell growth, we investigated at which level of the cell cycle this inhibition takes place. Fig. 3a shows that after 72 h of incubation, there was a significant increase in the number of cells at G2/M in cells treated with **Q7** + ASC (21.1% ± 1.85) compared to controls (16.4% ± 0.35). Conversely, when cells were incubated with **Q9** + ASC, a marked decrease (10.7% ± 3.10) was observed. These results suggest that the cell cycle is affected at the G2/M level. No changes in the distribution of cells were noted with shorter incubation times of 24 and 48 h (Supplementary Fig. 1S).

We further investigated whether the association of quinones + ASC affects some of the key proteins involved in cell cycle regulation, namely p53, p21, p27 and survivin (Fig. 3b). **Q7** alone or with ASC did not modify the expression of p53 or survivin, whereas the amounts of p27 and p21 were decreased at early incubation times. With longer incubation times (72 h), there was a slight trend to increased amounts of p21 but the relevance of this modification remains unclear. Regarding **Q9** alone or with ASC, the amounts of

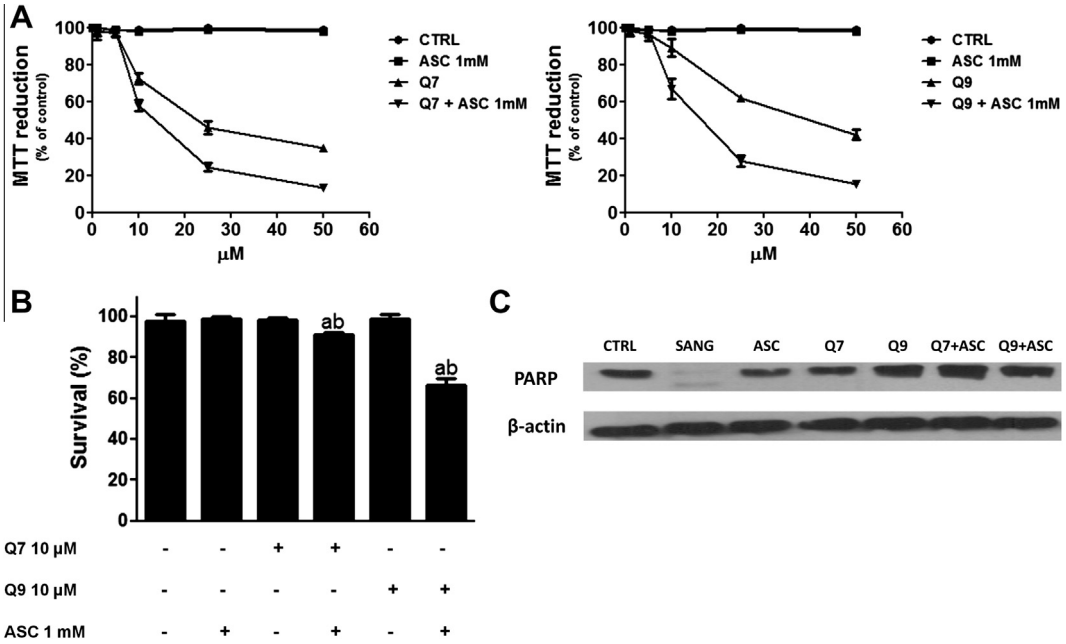


**Fig. 1.** Ascorbate-driven **Q7**/**Q9**-redox cycling impairs cell functionality and induces necrotic-like cell death in T24 cells. (A) Effects of **Q7** and **Q9** (1–50 μM) alone or with 1 mM ASC (24 h) on the ability of T24 cells to reduce MTT. (B) Effect of **Q7** and **Q9** (10 μM) on the viability of T24 cells (Trypan blue exclusion) incubated for 24 h with or without 1 mM ASC. (C) Effects of **Q7** and **Q9** on the integrity of PARP protein. Immunoblots were performed on whole cell homogenates after 24 h treatment with quinones alone (10 μM) or with 1 mM ASC, as reported in Section 2. Sanguinarine (SANG) at 5 μM was used for the positive control. Results are means ± SEM from three separate experiments. Statistical differences at $p < 0.05$ compared to untreated control cells (a) or between the treatments performed with quinone alone or with ASC (b).

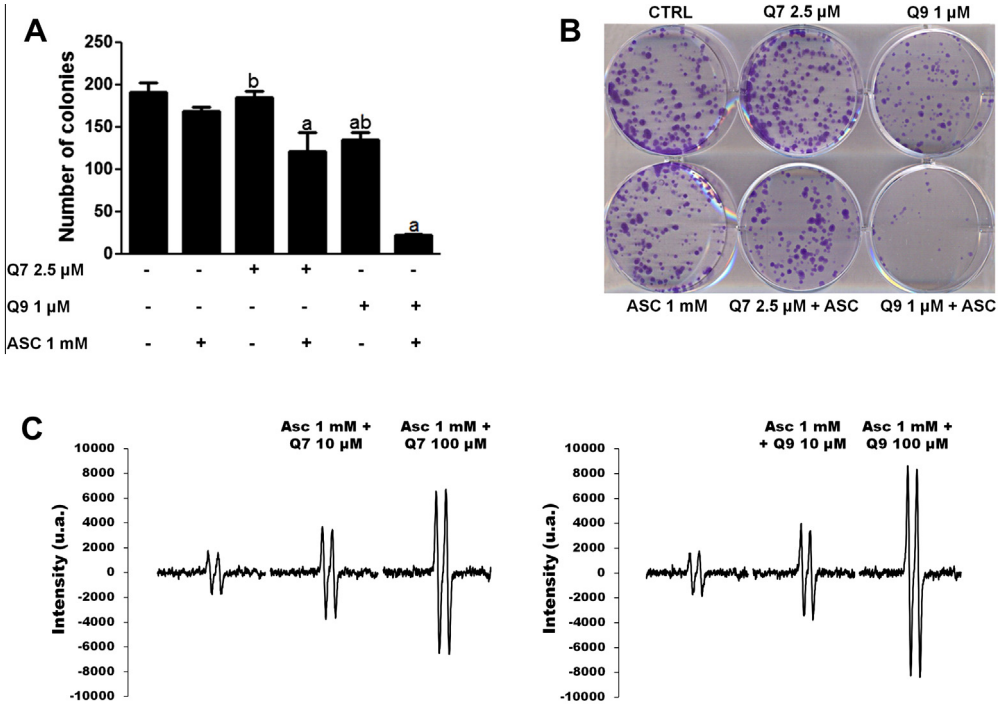


**Fig. 2.** Ascorbate-driven **Q7**/**Q9**-redox cycling inhibits T24 cell proliferation. (A, B) T24 cells were treated for 24 h with **Q7** (2.5 µM) and **Q9** (1.0 µM) alone or with ASC (1 mM). Cells were then washed with warm PBS, given fresh medium and allowed to grow for 10 days. Clonogenic survival was determined by staining colonies using crystal violet. (C) EPR spectra of free ascorbyl radical intensity in the presence of **Q7** or **Q9** (10 and 100 µM) alone or with 1 mM ASC. Results are means ± SEM from three separate experiments. Statistical differences at $p < 0.05$ compared to untreated control cells (a) or between the treatments performed with quinone alone or with ASC (b).

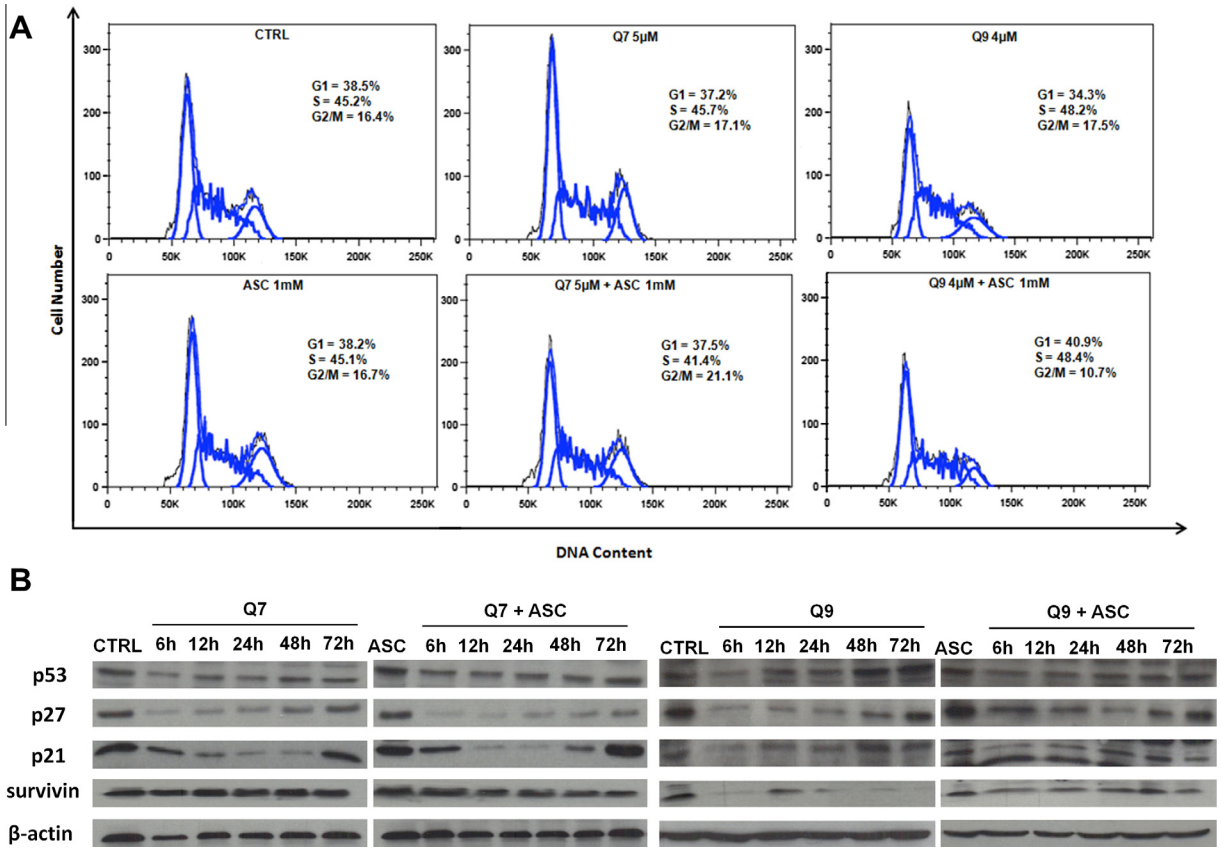


**Fig. 3.** Effects of quinones + ASC on cell cycle distribution and on key proteins regulating the cell cycle. Changes in T24 cell cycle progression induced by **Q7** (5.0 µM) or **Q9** (4.0 µM) alone or with 1 mM ASC for 72 h. Cells were pretreated with nocodazole (30 ng/ml, 14 h) prior to the treatments. (A) The percentage cell populations in G0/G1, S and G2/M were measured. (B) Effects of **Q7** (5.0 µM) or **Q9** (4.0 µM) alone or with 1 mM ASC on cell cycle protein markers. Immunoblots were performed after 6, 12, 24, 48 and 72 h-treatments.

all 4 proteins were generally decreased and, therefore, these proteins cannot be associated with the diminution in the number of cells in G2/M that we detected after 72 h (Fig. 3a).

### 3.3. Incubation of cells with quinones plus ASC reveals a senescent phenotype of T24 cancer cells but protein kinase inhibitors block progression to this senescent-like state

Fig. 4 shows the cytochemical detection of β-Gal activity, an enzyme activity only detected in senescent cells but not in pre-senescent, quiescent or immortal cells [17]. Indeed, a large number of cells were positively stained in cells incubated for 24 h with **Q9** alone or with ASC, (additional results of cells incubated with ASC alone or in the presence of **Q7** are shown in Supplementary Fig. 2S). In addition, T24 treated-cells appeared larger than those under control conditions. The count of β-Gal positive cells increased from 23% to 75% when comparing **Q9** alone to **Q9** + ASC. Fig. 4 also shows that the JNK inhibitor (SP600125) blocked the progression of cells to this senescent-like state, suggesting that MAPK may be involved in both senescence and cytotoxicity. Nevertheless, in cells incubated for 24 h with quinones + ASC in the presence of MAPK inhibitors (PD98054, SB202190 and SP600125), the cytotoxicity was slightly affected (Supplementary Fig. 3S). Regarding the MAPKs status in T24 cancer cells, it appears that **Q7** + ASC led to an activation of ERK1/2 but had little effects on JNK. Meanwhile, **Q9** + ASC induced the activation of stress pathways (p38 and JNK) but the degree of activation of ERK1/2 was the same as with **Q9** alone (Supplementary Fig. 3S).

## 4. Discussion

Since quinones can undergo redox cycling, we investigated their biological effects in the presence of ASC. We focused our study on cell proliferation, trying to identify the mechanisms underlying the inhibition of cell growth by quinones. We explored the points at which the cell cycle is arrested and hypothesized about a possible explanation as well as the consequences of such an effect.

Indeed, **Q7** and **Q9** are both cytotoxic against T24 cells, as shown by the dose-dependent inhibitory effect on metabolic competence and cell growth capacity. We observed that ASC strongly increased the cytotoxicity effects of both quinones. As expected, ASC enhanced quinone redox cycling as shown by the signal intensity of ascorbyl EPR spectra. From this result, **Q9** appears to be a better redox cycler than **Q7**. This finding may explain why **Q9**, at the same concentration (10 μM), induced necrotic-like cell death, as measured by cell counting using Trypan Blue exclusion. Indeed, neither **Q7** nor **Q9** were able to activate caspase-3, as shown by the absence of DEVDase activity and PARP cleavage.

Because of the strong inhibitory effect of the quinones on cell growth, we investigated their effects on the cell cycle. Quinones alone did not induce any changes in the number of cells at each cell cycle phase. However, in the presence of ASC, the most relevant effect was a substantial decrease in the number of cells at the G2/M phase. Western-blot analysis of p53, p21, p27 and survivin, all involved in the regulation of the cell cycle at different check-points, did not provide any information about a putative role of these proteins in cell growth inhibition by quinones.

A limitless replicative potential is one of the functional capabilities acquired by cancer cells during their development [18]. Cell cycle arrest thus represents an important barrier to cancer cell growth, which cells avoid in order to continue their proliferation. The observed morphological changes induced by quinones + ASC tend to associate the inhibition of cell growth (i.e., arrested cancer cells) with a senescent-like state. Indeed, interference in the cell cycle leads to senescence in cancer cells because cancer is a pro-senescent state and cell cycle arrest simply allows its manifestation [19]. In this context, the activation of growth-promoting pathways (i.e., MAPK and PI3K/mTOR) is one strategy cancer cells use to insure their development. Interestingly, these pathways are also involved in the senescent phenotype [20,21]. Our results show that **Q9** + ASC-treated cells displayed a senescent phenotype in which MAPKs, particularly p38 and JNK, may play a role. Since cellular senescence is believed to represent a natural tumor suppressor mechanism, senescence-inducing drugs may be effective (either

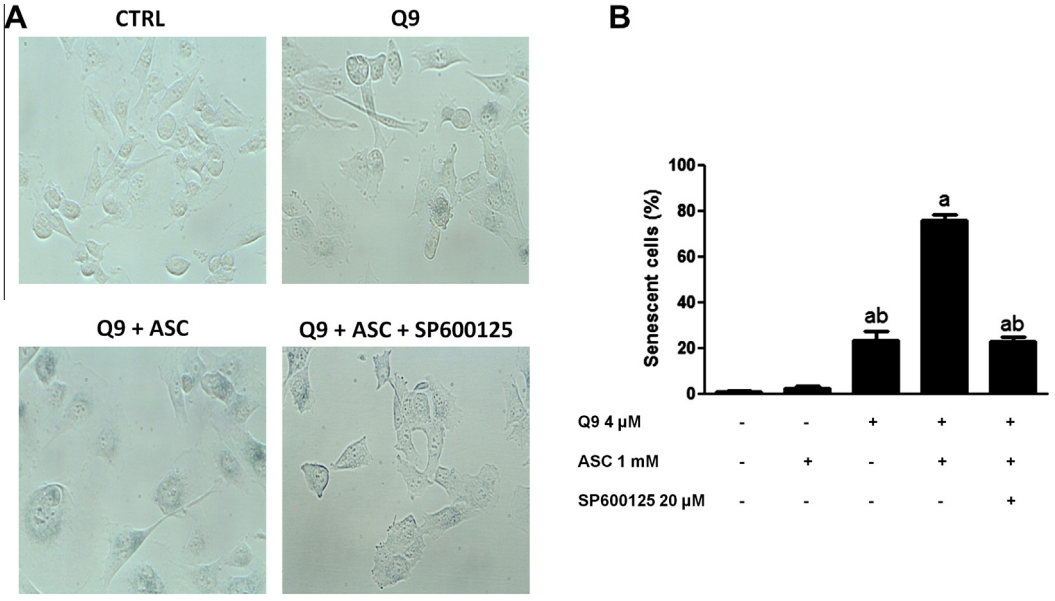


**Fig. 4.** Quinones + ASC reveal a senescent phenotype of T24 cells and SP600125, a JNK protein kinase inhibitor, blocks the progression to this senescent-like state. The figures represent cytochemical staining of T24 cells incubated for 24 h in the absence (control) and in the presence of **Q9** (4 μM), **Q9** (4 μM) + ASC (1 mM) and **Q9** (4 μM) + ASC (1 mM) + SP600125 (20 μM), respectively. Cells were counted as reported in Section 2. Results are means ± SEM from three separate experiments. Statistical differences at $p < 0.05$ compared to untreated control cells (a) or between the treatments performed with quinone alone or with ASC (b).

alone or combined with standard therapeutic approaches) to reduce tumor growth and limit toxicity to normal cells. On the other hand, confirming the induction of a senescent phenotype, it should be noted that cells treated with **Q7** or **Q9** alone or associated with ASC were resistant to apoptosis. Interestingly, although senescent cancer cells do not proliferate under oxidative stress, this implies that they may retain their metabolic capacities, facilitating cancer cell survival [22]. Nevertheless, this possibility is unlikely because cell impairment by quinones + ASC leads ultimately to cell death.

Finally, the difference in biological activity between **Q7** [2-(4-hydroxyanilino)-1,4-naphthoquinone] and **Q9** [2-(4-methoxyanilino)-1,4-naphthoquinone] can be attributed to the higher stabilization of the semiquinone radical species arising from reduction of **Q9** in the presence of ASC compared to the radical species generated from **Q7**. This assumption is supported by the half-wave potentials of **Q7** (−775 mV) and **Q9** (−856 mV), which reveal the stronger electron donating capacity of the 4-methoxyanilino group in **Q9** compared to the 4-hydroxyanilino substituent in **Q7**. It is interesting to note the influence of the stability of semiquinone radical species, which allows concentration levels to be maintained within the redox cycling process which are essential to support ROS generation. This fact, together with the higher lipophilicity of **Q9** ($\log P = 1.43$; **Q7** $\log P = 1.17$) probably favors a comparatively greater cellular uptake and ROS formation during the quinone redox cycling.

We conclude that redox cycler phenylaminonaphthoquinones inhibit the proliferation of cancer cells in the presence of ASC. This process involves a senescent cancer phenotype, which provokes changes in MAPK signaling pathways and impairs cell function, ultimately leading to necrotic cell death.

## Acknowledgments

This research was supported by the Belgian Fonds National de la Recherche Scientifique (FNRS), National Council for Scientific and Technological Development (CNPq) from Brazil and Fondo Nacional de Ciencia y Tecnología (Fondecyt Grant #1120050) from Chile. K.B. Felipe and M.R. Kviecisnki are fellows from the Brazilian Federal Agency for the Support and Evaluation of Graduate Education (CAPES). We thank Dr. S.N. Constantinescu and Dr. C. Pecquet for the gift of MAPK inhibitors and growth-promoting pathways analysis. We are also grateful to N. Dauguet for assistance with FACS analysis. Thanks to I. Blave, J.F. Gomes, P. Debluts, L. Gesché and V. Allaeys for their excellent technical support.

## Appendix A. Supplementary data

Supplementary data associated with this article can be found, in the online version, at http://dx.doi.org/10.1016/j.bbrc.2013.03.028.

## References

[1] A. Jemal, F. Bray, M.M. Center, et al., Global Cancer Statistics, CA Cancer J. Clin. 6 (2011) 69–90.
[2] Y. Octavia, C.G. Tocchetti, K.L. Gabrielson, et al., Doxorubicin-induced cardiomyopathy: from molecular mechanisms to therapeutic strategies, J. Mol. Cell. Cardiol. 52 (2012) 1213–1225.
[3] J. Benites, L. Rojo, J.A. Valderrama, et al., Part 1: anticancer activity of two euryfurylbenzoquinones on TLT, a murine hepatoma cell line. Role of vitamin C in the mechanism leading to cell death, Eur. J. Med. Chem. 43 (2008) 1813–1817.
[4] J. Benites, J.A. Valderrama, K. Bettega, et al., Biological evaluation of donor-acceptor aminonaphthoquinones as antitumor agents, Eur. J. Med. Chem. 45 (2010) 6052–6057.
[5] D. Rios, J. Benites, J.A. Valderrama, et al., Biological evaluation of 3-acyl-2-arylamino-1,4-naphthoquinones as inhibitors of Hsp90 chaperoning function, Curr. Top. Med. Chem. 12 (2012) 2094–2102.
[6] M. Kviecinski, R.C. Pedrosa, K.B. Felipe, et al., Inhibition of cell proliferation and migration by oxidative stress from ascorbate-driven juglone redox cycling in human bladder-derived T24 cells, Biochem. Biophys. Res. Commun. 421 (2012) 268–273.
[7] J. Verrax, M. Delvaux, N. Beghein, et al., Enhancement of quinone redox cycling by ascorbate induces a caspase-3 independent cell death in human leukaemia cells. An *in vitro* comparative study, Free Radic. Res. 39 (2005) 649–657.
[8] R. Beck, J. Verrax, N. Dejeans, et al., Menadione reduction by pharmacological doses of ascorbate induces an oxidative stress that kills breast cancer cells, Int. J. Toxicol. 28 (2009) 33–42.
[9] M. Torres, Mitogen-activated protein kinase pathways in redox signaling, Front Biosci. 8 (2003) 369–391.
[10] F. Esposito, R. Ammendola, R. Faraonio, et al., Redox control of signal transduction, gene expression and cellular senescence, Neurochem. Res. 29 (2004) 617–628.
[11] M.V. Chiantore, S. Vannucchi, G. Mangino, et al., Senescence and cell death pathways and their role in cancer therapeutic outcome, Curr. Med. Chem. 16 (2009) 287–300.
[12] T. Mosmann, Rapid colorimetric assay for cellular growth and survival: application to proliferation and cytotoxicity assays, J. Immunol. Methods 65 (1983) 55–63.
[13] R.I. Freshney, Freshney's Culture of Animal Cells – A Multimedia Guide CD-ROM, John Wiley & Sons Inc., New York, 1999.
[14] D.W. Nicholson, A. Ali, N.A. Thornberry, et al., Identification and inhibition of the ICE/CED-3 protease necessary for mammalian apoptosis, Nature 376 (2002) 37–43.
[15] V.M. Adhami, M.H. Aziz, H. Mukhtar, N. Ahmad, Activation of prodeath Bcl-2 family proteins and mitochondrial apoptosis pathway by sanguinarine in immortalized human HaCaT keratinocytes, Clin. Cancer Res. 9 (2003) 3176–3182.
[16] N.A.P. Franken, H.M. Rodermond, J. Stap, et al., Clonogenic assay of cells *in vitro*, Nat. Protocols 1 (2006) 2315–2319.
[17] G.P. Dimri, X. Lee, G. Basile, et al., A biomarker that identifies senescent human cells in culture and in aging skin in vivo, Proc. Natl. Acad. Sci. USA 92 (1995) 9363–9367.
[18] D. Hanahan, R.A. Weinberg, Hallmarks of cancer: the next generation, Cell 144 (2011) 646–674.
[19] M.V. Blagosklonny, Cell cycle arrest is not senescence, Aging 3 (2011) 94–101.
[20] J. Maruyama, I. Naguro, K. Takeda, H. Ichijo, Stress-activated MAP kinase cascades in cellular senescence, Curr. Med. Chem. 16 (2009) 1229–1235.
[21] P. Arivazhagan, D. Ayusawa, Cardiolipin activates MAP kinases during premature senescence in normal human fibroblasts, Biogerontology 8 (2007) 621–626.
[22] M. Collado, M. Serrano, Senescence in tumours: evidence from mice and humans, Nat. Rev. Cancer 10 (2010) 51–57.